doi:10.3788/gzxb20154404.0419001

海胆状金纳米粒子表面形貌对表面增强喇曼散射特性的影响

李军朋,周骏,姜涛,刘雁婷
(宁波大学 理学院 微电子科学与工程系,浙江 宁波 315211)

摘 要:采用改进的一步还原法合成了多种海胆状金纳米粒子,并对它们的表面增强喇曼散射特性与其表面形貌的关系进行了实验研究.实验表明,合成的海胆状金纳米粒子的直径及表面的尖刺大小可以通过改变加入到氯金酸溶液中的硝酸银的量来调节.当加入到氯金酸溶液中的硝酸银为 1μL 时,合成的海胆状金纳米粒子的直径最小而尖刺最长.同时测量的紫外-可见-近红外吸收光谱表明,海胆状金纳米粒子的局域表面等离子体共振带会随着加入到氯金酸溶液中的硝酸银量的增加而变宽.此外,通过喇曼标记分子对巯基苯甲酸(4MBA)的喇曼光谱测量发现,较小直径和较长尖刺的海胆状金纳米粒子具有更强的表面增强喇曼散射活性.

关键词:表面增强喇曼散射;局域表面等离子体;海胆状金纳米粒子;还原法
中图分类号:O433.4; O614.123 **文献标识码**:A **文章编号**:1004-4213(2015)04-0419001-5

SERS Characteristics of Sea Urchin-like Gold Nanoparticles Dependent on Their Surface Morphology

LI Jun-peng, ZHOU Jun, JIANG Tao, LIU Yan-ting
(*Department of Microelectronic Science and Engineering, Faculty of Science, Ningbo University, Ningbo, Zhejiang* 315211, *China*)

Abstract: A modified one-step reduction method was reported to synthesize the Sea Urchin-like Gold Nanoparticles (SU-GNPs), and the Surface-Enhanced Raman Scattering (SERS) characteristics of the SU-GNPs dependent on their surface morphology were experimentally studied. Experimental results shown that, the diameters and the thorn sizes of the SU-GNPs can be changed by adjusting the amount of silver nitrate aqueous solution added into hydrogen tetrachloroaurate trihydrate aqueous solution. When the added amount of silver nitrate was 1 μL, the as-prepared SU-GNPs had the longest thorns and the smallest diameter. And the measured UV-vis-NIR spectra exhibited that the localized surface plasmon resonance bands of the SU-GNPs were broaden with increasing of the added amount of silver nitrate. In addition, the effect of surface morphology on the SERS of SU-GNPs was investigated by using 4-mercaptobenzoic acid as a Raman reporter molecule. The results demonstrated that the SU-GNPs with smaller diameters and longer thorns gave rise to a stronger SERS enhancement.

Key words: Surface enhanced Raman scattering; Localized surface plasmon resonance; Sea urchin-like gold nanoparticles; reduction method
OCIS Codes: 190.5650; 160.4236; 160.4760; 240.6680; 240.6695; 300.6450

Foundation item: The National Natural Science Foundation of China (Nos. 61275153, 61320106014, and 11404177), the Natural Science Foundation of Zhejiang (No. LY12A04002), the International Collaboration Program of the Natural Science Foundation of Ningbo (Nos. 2010D10018 and 2012A610107)

First author: LI Jun-peng (1988—), male, graduate student, B.S. degree, mainly focus on, the synthesis of noble nanoparticles, surface enhancement Raman spectrum and their application in biosensing. Email:junpengddd@126.com
Responsible author(Corresponding author): ZHOU Jun (1958—), male, professor, Ph.D. degree, mainly focus on photonics, surface enhancement Raman spectrum and their applications in biosensing. Email:zhoujun@nbu.edu.cn

Received: Sep. 26, 2014; **Accepted**: Dec. 1, 2014

0 Introduction

In recent years, the research of Surface-Enhanced Raman Scattering (SERS) caused by Raman molecules deposited on rough noble metal surfaces become one of the hottest topics owing to their extensive application in the fields of biodetection, biomedicine, environmental monitoring, and analytical chemistry[1-5]. SERS originates from two mechanisms: chemical and electromagnetic enhancements. The former one comes from the enhanced field around the molecules adsorbed on the metallic surface due to the exchange of electrons in this charge-transfer system[6]. The latter one arises from the enhancement of the local electromagnetic field with the occurrence of Localized Surface Plasmon Resonance (LSPR) of noble metal nanostructure and is highly dependent on the size and shape of these metal nanoparticles[7]. Therefore, to reproducible and facilely fabricate noble nanoparticles with various sizes and morphologies are extremely crucial for practical application of the SERS techniques.

As we known, the analysis technique based on SERS spectroscopy is non-destructive and ultrasensitive, which requires to induce a relatively high SERS intensity by tailoring the noble metal nanostructure with a rough surface, especially on the junctions and sharp tips of these nanostructure which known as "hot spots" (a strong enhanced electromagnetic areas)[8-10]. For example, the different noble metal nanoparticles with various morphologies including flower[11], meatball[12], star[13], sea urchin[14], and hollow nanourchins[15] have been synthesized. However, it is still a challenge to achieve fine tuning surface morphology of these branched nanoparticles because of the inevitable influences of organic reducer during the synthesis process of the nanoparticles. Generally, cetyltrimethylammonium bromide (CTAB)[16], polyvinylpyrrolidone (PVP)[17], sodium dodecyl sulfate (SDS)[18], gelatin protein[19], or gum arabic[12] are usually used as the capping agent and stabilizer, but Ascorbic Acid (AA) as contrast partner, not only serves as an electron donor but also acts as a shape directing agent to induce the branched growth of nanostructures [20]. Thus, it is worth explored that a typical rough surface nanostructure such as Sea Urchin-like Gold Nanoparticles (SU-GNPs) is synthesized by AA in a way of green, simple, and low cost method.

In this article, we report a facile synthesis strategy for high-yield synthesis of sea urchin-like gold nanoparticles (SU-GNPs), that is, the SU-GNPs can be synthesized by directly adding AA into the mixed solution of silver nitrate aqueous solution and hydrogen tetrachloroaurate trihydrate aqueous solution. The major advantages of the proposed method are only one step growth process without firstly preparing gold or silver seed and no any capping agent or template to be used. Meantime, the surface morphologies of as-synthesized SU-GNPs can be tuned by just adjusting the amount added $AgNO_3$. And the optical characteristics of the SU-GNPs demonstrate the broadening of LSPR bands and SERS enhancement, which is significant to design a nano-biosensor with high sensitivity.

1 Experimental details

1.1 Chemicals

Silver nitrate ($AgNO_3$), and hydrogen tetrachloroaurate(Ⅲ) trihydrate ($HAuCl_4 \cdot 3H_2O$), were purchased from Sigma. Ascorbic acid (AA) was purchased from Bodi Chemical Reagent Co. (Tianjin, China). 4MBA were obtained from J&K Chemical. Milli-Q water (18.2MΩ cm resistivity) was used for all solution preparations. Glass wares were cleaned by aqua regia and rinsed with deionized water several times prior to the experiment.

1.2 Synthesis of SU-GNPs with 4MBA

A drop of $AgNO_3$(6 μL, 0.1 M) aqueous solution was firstly dissolved into 1 mL of $HAuCl_4$ (3 mM) aqueous solution with stirring for 5 seconds. Then, 1 mL of AA (10 mM) aqueous solution was immediately added into the above solution. After being stirred for a short period of time as about 20 seconds, dark gray suspension containing SU-GNPs formed. The above resulted precipitates were separated and washed by centrifugation with respectively using deionized water and absolute ethanol for several times to remove impurities. Finally the products were redispersed in 5 mL deionized water for further experiment.

In the synthesis process of SU-GNPs, the effect of $AgNO_3$ was studied by altering the amount of $AgNO_3$ from 0, 1, 2, 4, and 6 to 8 μL to obtain 6 samples, whereas the amount of $HAuCl_4$ and AA were fixed.

Furthermore, 20 μL of 4MBA was added to 5 mL of above sampler solutions under stirring and agitated for 5 h, respectively. Then, the unbound 4MBA molecules were removed by centrifugation at 9 000 rpm for 25 min, and the 4MBA-modified SU-GNPs settled on the bottom were redispersed in 5 mL deionized water. Next, the 4MBA-tagged SU-GNPs were dropped on Quartz glass and naturally dried for further SERS detection.

1.3 Measurements and instruments

The Scanning Electron Microscopy (SEM) and Transmission Electron Microscopy (TEM) images of the SU-GNPs were obtained by using FESEM (SU-70)

at an accelerating voltage of 5 kV and TEM (JEM-2100F JEOL) at an accelerating voltage of 200 kV, respectively. The optical absorption spectra of the SU-GNPs were recorded with a UV-vis-NIR spectrometer (Cary5000PC). The SERS properties of the SU-GNPs were examined by using the miniature Raman spectrometer (BWS415, B&W Tek Inc.) with a 785 nm semiconductor laser as the excitation source. The measurement parameters of the Raman spectrometer were set as follow: the laser power at the sample position was 49.55 mW and the accumulation time was 5 s; The scattered radiation was collected by a 40× objective lens with Numerical Aperture (NA) 0.65 and dispersed by the grating of 1 200 lines/mm, and then passed through a slit with 20 μm width to the Charge-Coupled Device (CCD) (2 048×2 048 pixels) detector. All the analysis was performed at room temperature.

2 Results and discussion

2.1 Characterization of SU-GNPs

The SEM and TEM images of the SU-GNPs synthesized with 6 μL $AgNO_3$ are shown in Fig. 1. From Fig. 1, the SU-GNPs were composed of a large number of thorns, and their average diameter and length of tips were calculated to be 250 and 50 nm, respectively. As a control sample without using of $AgNO_3$, we can see from Fig. 1(b), the nanoparticles only appear the irregular gold clusters with an average size of 150 nm. It presents the important role of $AgNO_3$ for forming the thorns of SU-GNPs.

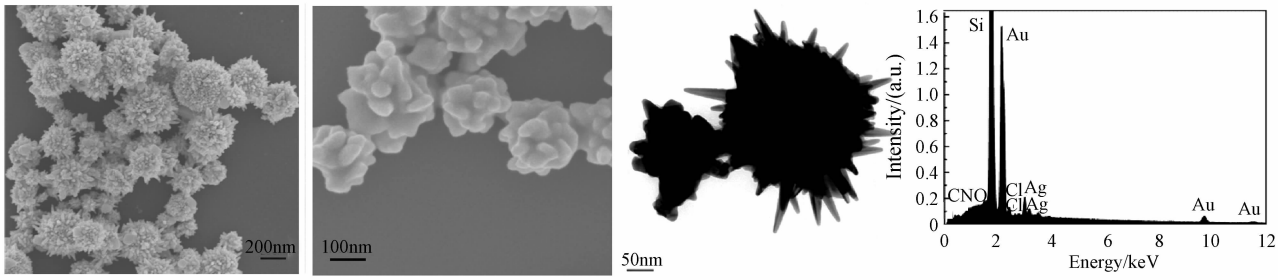

Fig. 1 The images of the GNPs and the EDS of the SU-GNPs

And, the chemical compositions of the SU-GNPs were analyzed by Energy-Dispersive Spectrometer (EDS) and shown in Fig. 1(d), which clearly displays the dominant peak of element gold, demonstrating that the samples are mainly composed of metallic gold. The element silver and chlorine are from the small amount of indiscerptible silver chloride (AgCl), and other elements are from the silica substrate and the derivatives of AA.

The current synthesis of SU-GNPs involved the template effect of the indiscerptible AgCl introduced by $AgNO_3$ in the aqueous solution of $HAuCl_4$. As described in Fig. 2, for the initial reaction solution, the $AgNO_3$ existed as ionic state together with the covalent bond between gold and chlorine. Then, the added AA broke such covalent bond, and the formed gold ions were immediately reduced into atoms, while the released chlorine anions combined with silver cation to created indiscerptible AgCl[21]. Next, AgCl compounds would attach to the surfaces of the growing gold atoms and acted as new nucleation cores, which sustained the further growth process and modified the final GNPs to exhibit a sea urchin-like morphology assembled with plentiful tiny spines.

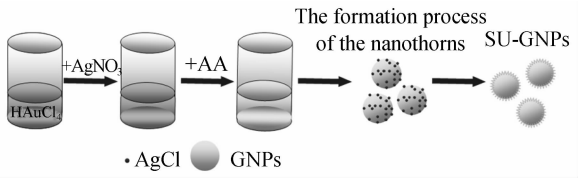

Fig. 2 The formation process of the SU-GNPs

According to the above analysis about the formation process of the thorns, it can be known that the number of branches of the SU-GNPs can be widely tailored by controlling the amount of the $AgNO_3$ aqueous solution which adds into the $HAuCl_4$ aqueous solution. As shown in Fig. 3, the amount of $AgNO_3$ aqueous solution was selectively regulated from 1 μL to 8 μL under fixing other synthetic conditions. Fig. 3(a) shows that the sample synthesized with 1 μL $AgNO_3$ aqueous solutions is a small gold core assembled of a lot of large and long spikes, which origin from a few indiscerptible AgCl attach themselves to the growing gold atoms and act as new cores. The diameters of the gold core were calculated to be about 100 nm and the lengths of the spikes were about 150 nm. The gold core is becoming bigger and bigger, the spikes shorten and bestrew with the gold core with increasing of the $AgNO_3$, as shown in Fig. 3(b), 3(c), 3(d) and 3(e).

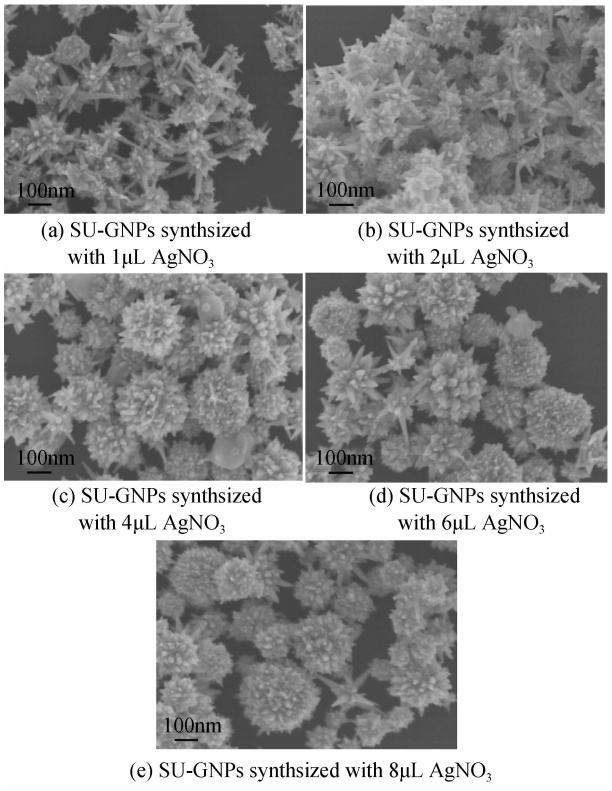

Fig. 3 SEM images of the SU-GNPs prepared with different amount of $AgNO_3$

In addition, from Fig. 3(d) and 3(e), we can see that the SU-GNPs synthesized with 6 and 8 μL $AgNO_3$ aqueous solutions are almost the same. It is probably because that more and more spikes appear and bestrew with the gold core, then the growing gold atoms connect each other to form a new layer around the indiscerptible AgCl. Therefore, the $AgNO_3$ amount controlling the supply of the indiscerptible AgCl in the reaction system is a crucial factor for generating variation sizes and morphologies of the SU-GNPs.

Fig. 4 shows the UV-vis-NIR absorption spectra of the SU-GNPs in aqueous solution. In the case without $AgNO_3$, the LSPR bands obvious distinct from the LSPR of SU-GNPs synthesized with $AgNO_3$. And the LSPR bands gradually broaden with the increase of the $AgNO_3$ amount in the beginning, but keep almost invariant with the further increasing $AgNO_3$ amount. From Fig. 5, we can clearly see the changes in morphology of the SU-GNPs. The LSPR bands are gradually broaden because of the growth of the gold core and the decrease of the spikes. And the LSPR peak around 980 nm can be attributed to the multipolar plasmon modes induced by the geometric asymmetry of the SU-GNPs[22]. According to Refs [23] and [24], the size, shape and dielectric environment have a considerable effect on optical properties of GNPs, of course, will certainly affect that of the synthesized SU-GNPs. Thus, the varying of $AgNO_3$ amounts lead to the different structures and shapes of SU-GNPs, which will result in a variety of their absorption spectra.

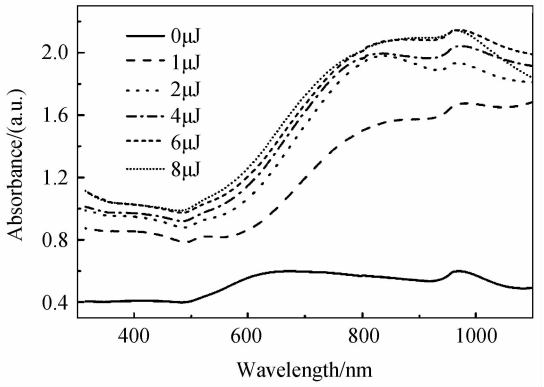

Fig. 4 UV-Vis-NIR absorption spectra of the SU-GNPs prepared with different amounts of $AgNO_3$ aqueous solutions at 0, 1, 2, 4, 6, and 8 μL

2.2 SERS performance of SU-GNPs

To understand the SERS performances of the synthesized SU-GNPs depended on their size and morphology, the Raman spectra of the 4MBA-tagged SU-GNPs synthesized with different amount of $AgNO_3$ were measured and shown in Fig. 5. We can see from Fig. 5, the fingerprint bands of 4MBA have strong intensities which indicate the SERS enhancement characteristic of SU-GNPs. The two dominant peaks at 1 076 and 1 586 cm^{-1} are assigned to the ring breathing modes. The Raman band at 849 cm^{-1} is attributed to the COO^- bending mode ($\delta(COO^-)$) and that at 1 144 cm^{-1} originates from a mixed mode ($13\beta(CCC)+\nu(C-S)+\nu(C-COOH)$). Besides, the one at 1 432 cm^{-1} is ascribed to the ν_s (COO^-) stretching mode[25]. It can be clearly observed in Fig. 5, all of the fingerprint bands of 4MBA have same peak positions, but their peak intensities are obviously different. That is, with decreasing the amount of $AgNO_3$, the SERS intensities of the synthesized 4 MBA-tagged SU-GNPs gradually increase and reached the highest intensity at the case of 1 μL $AgNO_3$ aqueous solution. And as a control sample , the GNPs synthesized without $AgNO_3$

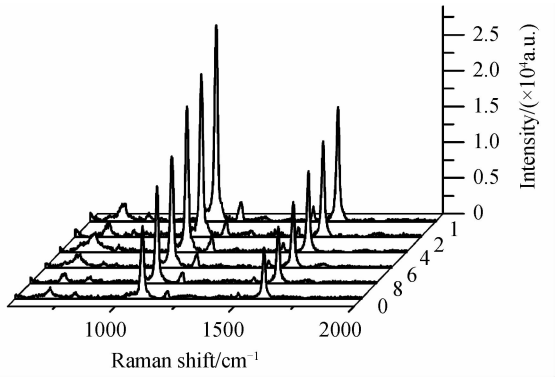

Fig. 5 Raman spectra of 4MBA-tagged SU-GNPs synthesized with different amount of $AgNO_3$: 0, 1, 2, 4, 6, and 8 μL

has the smallest intensity. It demonstrates that the SU-GNPs with longer thorns can exhibit excellent SERS performances.

We also investigated the reproducibility of the SERS signals of the SU-GNPs synthesized with 1 μL $AgNO_3$ by randomly choosing ten probe sites on the SERS substrates. From Fig. 6, we can see very small difference among the ten SERS signals. It demonstrated that the SERS substrates have excellent SERS reproducibility.

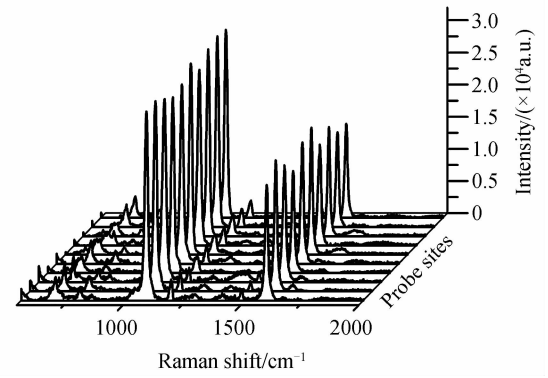

Fig. 6 The Raman spectra of the 4MBA-tagged SU-GNPs at different probe sites on the SERS substrate

3 Conclusion

In a word, a modified one-step reduction method has been exploited to synthesize SU-GNPs for SERS application. The surface morphologies of the SU-GNPs have been tuned by altering the added amount of $AgNO_3$ aqueous solution. And the absorption bands of SU-GNPs widen with the increase of the $AgNO_3$ amounts. The experimental results show the SU-GNPs with longer thorns have a superior SERS performance, which is of great importance to develop a high-sensitive biosensor applied in immunoassay.

References

[1] MICHAELS A M, NIRMAL M, BRUS L E. Surface enhanced Raman spectroscopy of individual rhodamine 6G molecules on large Ag nanocrystals [J]. *Journal of the American Chemical Society*, 1999, **121**(43): 9932-9939.

[2] ANKER J N, HALL W P, LYANDRES O, *et al*. Biosensing with plasmonic nanosensors[J]. *Nature Materials*, 2008, **7**(6): 442-453.

[3] LI J F, HUANG Y F, DING Y, *et al*. Shell-isolated nanoparticle-enhanced Raman spectroscopy[J]. *Nature*, 2010, **464**(7287): 392-395.

[4] SMYTHE E J, DICKEY M D, BAO J M, *et al*. Optical antenna arrays on a fiber facet for in situ Surface-Enhanced Raman scattering detection[J]. *Nano Letters*, 2009, **9**(3): 1132-1138.

[5] QIAN X M, PENG X H, ANSARI D O, *et al*. In vivo tumor targeting and spectroscopic detection with surface-enhanced Raman nanoparticle tags[J]. *Nature Biotechnology*, 2008, **26**(1): 83-90.

[6] XIA Y N, XIONG Y J, LIM B, *et al*. Shape-controlled synthesis of metal nanocrystals: simple chemistry meets complex physics [J]. *Angewandte Chemie International Edition*, 2009, **48**(1): 60-103.

[7] MOSKOVITS M. Surface-enhanced spectroscopy[J]. *Reviews of Modern Physics*, 1985, **57**(3): 783-826.

[8] SMITH W E. Practical understanding and use of surface enhanced Raman scattering/surface enhanced resonance Raman scattering in chemical and biological analysis [J]. *Chemical Society Reviews*, 2008, **37**(5): 955-964.

[9] HUH Y S, CHUNG A J, ERICKSON D. Surface enhanced Raman spectroscopy and its application to molecular and cellular analysis[J]. *Microfluidics and Nanofluidics*, 2009, **6**(3): 285-297.

[10] BELL S E J, SIRIMUTHU N M S. Quantitative surface-enhanced Raman spectroscopy [J]. *Chemical Society Reviews*, 2008, **37**(5): 1012-1024.

[11] WANG X X, YANG T, LI X, *et al*. Three-step electrodeposition synthesis of self-doped polyaniline nanofiber-supported flower-like Au microspheres for high-performance biosensing of DNA hybridization recognition[J]. *Biosensors and Bioelectronics*, 2011, **26**(6): 2953-2959.

[12] WANG H, HALAS N J. Mesoscopic Au "meatball" particles [J]. *Advanced Materials*, 2008, **20**(4): 820-825.

[13] KUMAR P S, PASTORIZA-SANTOS I, *et al*. High-yield synthesis and optical response of gold nanostars [J]. *Nanotechnology*, 2008, **19**(1): 015606.

[14] XU F G, CUI K, SUN Y J, *et al*. Facile synthesis of urchin-like gold submicrostructures for nonenzymatic glucose sensing [J]. *Talanta*, 2010, **82**(5): 1845-1852.

[15] LIU Z, YANG Z B, PENG B, *et al*. Highly sensitive, uniform, and reproducible surface enhanced Raman spectroscopy from hollow Au-Ag alloy nanourchins [J]. *Advanced Materials*, 2014, **26**(15): 2431-2439.

[16] CHEN S H, WANG Z L, BALLATO J, *et al*. Monopod, bipod, tripod, and tetrapod gold nanocrystals[J]. *Journal of the American Chemical Society*, 2003, **125**(52): 16186-16187.

[17] LIANG H Y, LI Z P, WANG W Z, *et al*. Highly surface-roughened "flower-like" silver nanoparticles for extremely sensitive substrates of surface-enhanced Raman scattering[J]. *Advanced Materials*, 2009, **21**(45): 4614-4618.

[18] KUO C H, HUANG M H. Synthesis of branched gold nanocrystals by a seeding growth approach[J]. *Langmuir*, 2005, **21**(5): 2012-2016.

[19] LU L H, AI K L, OZAKI Y. Environmentally friendly synthesis of highly monodisperse biocompatible gold nanoparticles with urchin-like shape[J]. *Langmuir*, 2008, **24**(3): 1058-1063.

[20] WANG L, HU C, NEMOTO Y, *et al*. On the role of ascorbic acid in the synthesis of single-crystal hyperbranched platinum nanostructures[J]. *Crystal Growth Dsign*, 2010, **10**(8): 3454-3460.

[21] YUAN H, MA W H, CHEN C C, *et al*. Shape and SPR evolution of thorny gold nanoparticles promoted by silver ions [J]. *Chemistry of Materials*, 2007, **19**(7): 1592-1600.

[22] WU D J, JIANG S M, CHENG Y, *et al*. Fano-like resonance in symmetry-broken gold nanotube dimer [J]. *Optics Express*, 2012, **20**(24): 26559-26567.

[23] SUN Y G, XIA Y N. Mechanistic study on the replacement reaction between silver nanostructures and chloroauric acid in aqueous medium [J]. *Journal of the American Chemical Society*, 2004, **126**(12): 3892-3901.

[24] LU X, TUAN H Y, CHEN J, *et al*. Mechanistic studies on the galvanic replacement reaction between multiply twinned particles of Ag and $HAuCl_4$ in an organic medium [J]. *Journal of the American Chemical Society*, 2007, **129**(6): 1733-1742.

[25] RE LU E C, BLACKIE E, MEYER M, *et al*. Surface enhanced raman scattering enhancement factors: a comprehensive study[J]. *Journal of Physics Chemical C*, 2007, **111**(37): 13794-13803.